

Alma Mater Studiorum Università di Bologna
Archivio istituzionale della ricerca

The use of multiparametric 18F-fluoro- L -3,4-dihydroxy-phenylalanine PET/MRI in post-therapy assessment of patients with gliomas

This is the final peer-reviewed author's accepted manuscript (postprint) of the following publication:

Published Version:

Fraioli F., Shankar A., Hyare H., Ferrazzoli V., Militano V., Samandouras G., et al. (2020). The use of multiparametric 18F-fluoro- L -3,4-dihydroxy-phenylalanine PET/MRI in post-therapy assessment of patients with gliomas. NUCLEAR MEDICINE COMMUNICATIONS, 41(6), 517-525 [10.1097/MNM.0000000000001184].

Availability:

This version is available at: <https://hdl.handle.net/11585/871841> since: 2022-02-28

Published:

DOI: <http://doi.org/10.1097/MNM.0000000000001184>

Terms of use:

Some rights reserved. The terms and conditions for the reuse of this version of the manuscript are specified in the publishing policy. For all terms of use and more information see the publisher's website.

This item was downloaded from IRIS Università di Bologna (<https://cris.unibo.it/>).
When citing, please refer to the published version.

(Article begins on next page)

This is the accepted manuscript of:

Fraioli F, Shankar A, Hyare H, Ferrazzoli V, Militano V, Samandouras G, Mankad K, Solda F, Zaccagna F, Mehdi E, Lyasheva M, Bomanji J, Novruzov F.

The use of multiparametric 18F-fluoro-L-3,4-dihydroxy-phenylalanine PET/MRI in post-therapy assessment of patients with gliomas.

Nucl Med Commun. 2020 Jun;41(6):517-525

The final published version is available online at: <https://doi.org/10.1097/mnm.0000000000001184>

Rights / License:

The terms and conditions for the reuse of this version of the manuscript are specified in the publishing policy. For all terms of use and more information see the publisher's website.

This item was downloaded from IRIS Università di Bologna (<https://cris.unibo.it/>)

When citing, please refer to the published version.

The use of Multiparametric ^{18}F -DOPA PET/MRI in post-therapy assessment of patients with gliomas.

Francesco Fraioli¹, Ananth Shankar², Harpreet Hyare^{3,4}, Valentina Ferrazzoli⁵, Vincenzo Militano¹, George Samandouras⁶, Khsitij Mankad⁷, Francesca Solda⁸, Fulvio Zaccagna⁹, Elnur Mehdi¹⁰, Maria Lyasheva¹, Jamshed Bomanji¹ & Fuad Novruzov^{1,10}

¹ *Institute of Nuclear Medicine, University College London Hospitals NHS Foundation Trust, UK.*

² *Department of Pediatric & Adolescent Oncology, University College London Hospitals NHS Foundation Trust, UK.*

³ *Imaging Department, University College London Hospital NHS Foundation Trust, London, UK.*

⁴ *Department of Brain Repair and Rehabilitation, UCL Institute of Neurology, London, UK*

⁵ *Department of Biomedicine and Prevention, University of Tor Vergata, Rome, Italy*

⁶ *Victor Horsley Department of Neurosurgery, National Hospital for Neurology and Neurosurgery, University College London Hospitals NHS Foundation Trust, London, UK*

⁷ *Department of Radiology, Great Ormond Street Hospital NHS Foundation Trust, London, UK*

⁸ *Department of Oncology, University College London Hospitals NHS Foundation Trust, London, UK*

⁹ *Department of Radiology, University of Cambridge School of Clinical Medicine, Cambridge, UK*

¹⁰ *Nuclear Medicine Department at Azerbaijan National Centre of Oncology. Baku, Azerbaijan*

Word counts: 3194

Corresponding Author

Francesco Fraioli, MD, PhD

University College London Hospitals UCL(H)

235 Euston Rd

London, NW1 2BU

Tel. +447544460731

Abstract

Purpose: To determine the utility of ^{18}F -DOPA PET/MRI versus cross-sectional MRI alone in glioma response assessment and identify whether the two techniques demonstrate different tumour features.

Methods: ^{18}F -DOPA PET/MRI studies from 40 patients were analysed. Quantitative PET parameters and conventional MRI features were recorded. Tumour volume was assessed on both PET and MRI. Using DSC-PWI, maps of CBF and CBV were obtained. Within VOIs of tumour features and normal-appearing white matter (NAWM) drawn on MRI, SUV_{max} , CBF and CBV were recorded. Presence of residual active tumour was assessed by qualitative visual assessment. ROC analysis was performed univariately and on parameter combination to analyse ability to determine presence/absence of disease. Reference standard for presence of viable tissue was biopsy or clinical follow-up.

Results: Median SUV_{max} was 3.4 for low-grade glioma (LGG) and 3.3 for high-grade glioma (HGG). There was a significant correlation between PWI parameters and WHO grade ($p < 0.001$), but no correlation with SUV_{max} . Median ^{18}F -DOPA volume was 8216.88 mm^3 for HGG and 6284.94 mm^3 for LGG; MRI volume was 6316.57 mm^3 and 5931.55 mm^3 respectively. SUV_{max} analysis distinguished enhancing and non-enhancing components from necrosis and NAWM and demonstrated active disease in non-enhancing regions. Visually, the modalities were concordant in 37 patients. Combining the multiparametric PET/MRI approach with all available data enhanced detection of the presence of tumour (AUC 0.99, $p < 0.01$).

Conclusion: MRI and ^{18}F -DOPA are complementary modalities for assessment of tumour burden. Matching ^{18}F -DOPA and MRI in assessing residual tumour volume may better delineate the radiotherapy target volume.

Introduction

Structural magnetic resonance imaging (MRI) is the current standard for detection and follow-up of brain tumours of any grade and histology. Although the Response Assessment in Neuro-Oncology RANO criteria [1–3] take into account non-enhancing disease, response assessment still relies on axial bi-dimensional measurements of the enhancing tumour on conventional contrast-enhanced T1-weighted images [4]. With the advent of new radiotherapy programmes such as proton beam therapy and chemotherapy protocols, evaluation of post-treatment glioma burden is mandatory to optimise and personalise treatments [5]. The need for additional insights into tumour biology and infiltrative behaviour has prompted the increasing use of radionuclide PET imaging and advanced MRI techniques, such as perfusion-weighted imaging (PWI), diffusion-weighted imaging (DWI) with advanced modelling (e.g. NODDI or VERDICT) and magnetic resonance proton spectroscopy [6–8]. Positron emission tomography (PET) imaging with the amino acid tracer 6-¹⁸F-fluoro-L-3,4-dihydroxy-phenylalanine (¹⁸F-DOPA) has the ability to provide additional information in brain tumours over conventional cross-sectional contrast-enhanced computed tomography (CT) or MRI alone [9].

Previous studies comparing PET and MRI have reported that the two techniques can correlate with different biological characteristics of the brain [10–11]. Tracer uptake with ¹⁸F-DOPA PET reflects amino acid metabolism within the tumour cells, while gadolinium MRI reflects the disruption of the blood-brain barrier and the remodelled vascular network within the tumour [12]. Therefore, we believe that the simultaneous acquisition of ¹⁸F-DOPA PET and gadolinium-enhanced MRI can provide better insights on the tumour biology as compared to a single-modality approach thanks to the capability of exploiting different intrinsic, complimentary, biological features. Despite the complementary nature of the two techniques, hitherto, few reports have investigated the value of multimodality imaging for glioma response assessment using a hybrid PET/MRI system [13–14]; thus, the primary aim of our study was to assess the potential benefit of a hybrid ¹⁸F-DOPA PET/MRI versus cross-sectional MRI for the evaluation of active disease in post-treatment patients. Our secondary aim was to recognise whether the two techniques show different features of the tumour.

This assessment has a clinical impact not only because it helps in the understanding of the biological behaviour of glioma but also because it allows better identification of tumour burden and personalised treatment planning.

Materials and Methods

Patient population and treatment

Forty consecutive patients [median age 34 years (5–65 years), M:F 23:17] diagnosed with glioma who were undergoing treatment and had been referred for brain ^{18}F -DOPA PET/MRI were prospectively recruited after securing informed consent from the patient or from parents or the legal guardian. Imaging using the hybrid 3T PET/MRI scanner was approved by the local ethics committee. All investigations were carried out in accordance with the Declaration of Helsinki.

Patient demographics, including WHO grading of tumour and treatment modalities, are shown in Table 1.

Histopathological categorisation of the tumours was done as per the 2016 WHO classification [15], including molecular criteria that occasionally supplanted morphology and grade of the tumour.

Chemotherapy regimens varied according to tumour histology. Radiotherapy doses ranged between 50 and 54 Gy in 30 fractions over a 6-week period. The median time between the end of treatment and ^{18}F -DOPA PET/MRI was 8 months (5–12 months). Tumour histopathology was confirmed after surgical tumour resection or by biopsy of the tumour. The reference standard for assessing residual/recurrent tumour was tumour biopsy, where possible, or clinical-radiological follow-up.

Imaging

All PET/MRI studies were conducted on a hybrid 3T clinical scanner (Siemens mMR biograph, Siemens Healthcare, Erlangen, Germany) at our institution.

Static PET acquisitions were post-reconstructed at the 15th minute (0–15 min) after injection of ^{18}F -DOPA (dose range 250–370 MBq, according to body weight) [16]. Based on scatter and attenuation correction images, standardised uptake value (SUV) images were calculated, accounting for time between injection and acquisition and the ^{18}F half-life.

MRI sequences included coronal and axial T2-weighted (T2-W) inversion-recovery acquisition (FLAIR; TE 397 ms, TR 5000 ms, TI 1800 ms, TA 5.50 min, voxel size

1.1×1.1×1.1 mm), axial T2-W TSE imaging (TE 300 ms, TR 4000 ms, TA 3.50 min, slice thickness 4 mm) and an axial T1-W 3D isovolumetric interpolated breath-hold examination before and after gadolinium (0.2 ml/kg) injection (TE 3.8 ms, TR 2000 ms, TA 5.00 min, voxel size 1.1×1.1×1.1 mm).

Dynamic susceptibility contrast perfusion-weighted imaging (DSC-PWI) MRI was acquired after a preload dose (PLD) administration of gadolinium-based contrast agent (GBCA) (0.005–0.1 mmol/kg) that allowed the acquisition of PLD-corrected data in order to partially correct for GBCA extravasation-induced T1 effects. DSC-PWI data (gradient-echo echo-planar imaging with TR/TE/flip angle 1500–2000 ms/20 ms/60°, FOV 24×24 cm, matrix 128×128, 5-mm slice thickness, no gap) were acquired during 3 min with the bolus injection occurring at 1 min after the start of the DSC sequence.

Image analysis

Two nuclear medicine physicians in consensus recorded several quantitative PET parameters [SUV_{max} , target-to-background ratio (T/B) and target-to-striatum (T/S) ratio].

For visual analysis, the lesion was considered positive for recurrence when ^{18}F -DOPA uptake in the suspicious area was greater than the uptake in the adjacent normal tissue. Two neuroradiologists in consensus recorded the maximal diameters, tumour enhancement (graded qualitatively as low, medium or high and in percentage terms using a five-point scale: 0: 1: <5%; 2: 6%–33%; 3: 34%–66%; 4: 67%–95%; 5: >95% [17]; VASARI project – wiki.cancerimagingarchive.net) and tumour features (enhancing, non-enhancing and necrosis). To obtain cerebral perfusion maps (CBV and CBF), a semi-automated arterial input function method derived from a region of interest (ROI) located close to the middle cerebral artery, contralateral to the lesion side, was used [image analysis was carried out using commercial software (IB Neuro v1.1; Imaging Biometrics, LLC, Elm Grove, WI)]. A circular ROI (size range 30–50 pixels) encompassing the lesion was drawn to measure the maximum CBV and CBF, avoiding necrotic areas and non-tumour microvasculature. The relative CBV and CBF were then calculated for each lesion by dividing the tumour CBV and CBF by the mean CBV/CBF values obtained from a similar ROI (same size range) placed in the contralateral normal-appearing white matter in order to normalise values within each patient.

In a second reading session, the same pair of readers, blinded to the other modality, manually determined the volume of tumour (VOI) on a dedicated platform (ITK-SNAP) on areas of

maximal visual uptake on PET (^{18}F -DOPA_{vol}) and enhancement/signal change in the tumour on MRI (MRI_{vol}).

In addition to outlining the whole tumour volume, the two neuroradiologists determined separate VOIs based on specific tumour features (enhancing, non-enhancing and necrotic components). Within these VOIs [with the help of a dedicated computing programme (Matlab, Mathworks)], SUV_{max} values were recorded after carefully ensuring perfect co-registration of the images.

Finally, in consensus, and blinded to the previous patient history and results of the other imaging modality, radiologists and nuclear medicine physicians were asked to grade on a five-point scale of confidence the presence of residual active tumour using a qualitative visual assessment: 1 = no tumour; 2 = tumour presence unlikely, 3 = possible presence of viable tumour, 4 = likely presence of viable tumour, 5 = definite tumour presence. Radiologists had all the MRI sequences acquired during the PET/MRI study available and the nuclear medicine physicians had both the PET and the anatomical sequences. To compare the two modalities, the five-point scale was dichotomised as follow: grades 1 and 2 were classified as absence of tumour and grades 3, 4 and 5 were considered to indicate presence of tumour.

Statistical analysis

Statistical analysis was performed using commercially available SPSS 17 and RStudio version 1.1.463 (RStudio Inc., Boston, MA) for Macintosh based on R version 3.5.1 (The R Foundation for Statistical Computing Platform). The association between metabolism, enhancement, size, CBV, total and specific volumes and overlapping between the two modalities for high- and low-grade gliomas was evaluated by non-parametric correlation analysis using the Spearman rank correlation coefficient (ρ). For all statistical analyses, a two-tailed p value of less than 0.05 was considered to indicate a statistically significant difference; however, a Bonferroni correction was applied to avoid any bias deriving from multiple comparisons. Therefore, all the significant p values reported in the results are post Bonferroni correction.

The single modalities and the combination of the two modalities were analysed for their ability to determine presence/absence of disease using ROC analysis, and the area under the curve (AUC) was calculated.

Results

PET/MRI examinations were completed in all patients with a mean PET/MRI scan time (including room time) of 25 ± 3 min (the simultaneous PET acquisition was performed during the first part of the MRI scan). A descriptive summary of MRI features and PET parameters is shown in Table 2.

Lesion sizes on MRI were recorded in all patients and varied (longest axes) between 7.00 and 82.20 mm (median 31.85 mm). Twenty-six lesions (65%) demonstrated substantial contrast enhancement on MRI (no contrast enhancement in 11 cases, less than 5% in 3, 6%–33% in 6, 34%–67% in 9, 67%–95% in 6 and >95% in 5). All 40 patients demonstrated T2 signal change and 19 showed a necrotic core/component.

The median SUV_{max} , T/S and T/N for LGG and HGG are shown in Table 2. No significant correlation was found between tumour size and SUV_{max} (longest size: $p=0.1038$) or between degree of enhancement and SUV_{max} ($p=0.0602$), T/N ($p=0.1792$) or T/S ($p=0.1245$). The median SUV_{max} , T/S and T/N for patients with non-enhancing and patients with enhancing lesions are shown in Table 3.

Volumes derived from ^{18}F -DOPA and MRI are shown in Table 2. Significant differences in volume for LGG and for HGG were recorded between ^{18}F -DOPA PET and MRI ($p=0.02$ and $p=0.0002$ respectively), with both LGG and HGG being bigger at ^{18}F -DOPA PET. The percentage of overlap was significantly higher for LGGs than for HGGs ($p=0.0002$).

The overlap areas between the tumours were 60% [IQR 53%–69%] for HGGs and 80% [IQR 72%–84%] for LGGs (example in Figure 1).

A significant correlation was found between CBF and CBV for WHO grading (CBF_{mean} and CBV_{mean} : $p<0.001$; CBF_{max} and CBV_{max} : $p<0.001$; CBF_{mean} and CBV_{max} : $p<0.001$; CBF_{max} and CBV_{mean} : $p<0.001$) but no correlation was found between SUV_{max} and perfusion parameters for all WHO grading of glioma (CBV_{mean} : $p=0.1825$; CBV_{max} : $p=0.2296$; CBF_{mean} : $p=0.3978$; CBF_{max} : $p=0.5713$). Correlations for size of tumour (longest and perpendicular), SUV_{max} , T/N, T/S, degree of enhancement, CBV_{mean} , CBV_{max} , CBF_{mean} and CBF_{max} are shown in Figure 2.

The quantitative assessment of ^{18}F -DOPA uptake within the areas of different tumour components plotted against DSC-PWI is shown in Figure 3.

Visually both modalities were concordant in 37 patients; the three discordant cases comprised two LGG and one HGG (two were positive on MRI but negative on PET while one was positive on PET but negative on MRI). Examples of discordance for both modalities are shown in Figures 4 and 5). The reference standard (surgical biopsy) demonstrated presence of tumour in all cases.

Single-modality analysis of PET imaging demonstrated an area under the curve (AUC) of 0.94 ($p<0.03$) (Figure 6f in supplemental material). Perfusion MR imaging with dynamic susceptibility contrast resulted in an AUC of 0.94 ($p=0.03$). Combining structural MRI and perfusion showed increased value in detecting presence of tumour: the AUC in ROC analysis was 0.97 ($p<0.02$). ROC analysis using a combined multiparametric PET/MRI approach with all the available data resulted in an AUC of 0.99 ($p<0.01$).

Discussion

One of the main challenges in assessing treatment response in gliomas lies in establishing the presence of active residual tumour, which often requires several MRI follow-up scans. MRI scans performed in the first 12 weeks of treatment can be difficult to interpret as pseudo-response/progression can mimic true progression. Furthermore, evaluation of the tumour burden is crucial for planning a more targeted/tailored treatment that is centred on the most viable tumour component.

In this study, we present the correlation between different PET and MRI parameters in a series of scans performed for post-treatment response assessment. Our results confirm the hypothesis that the two modalities evaluate different functional characteristics of glioma. MRI mainly focuses on the disruption of the blood-brain barrier on post-contrast T1W images and the infiltrative growth pattern of tumours on T2-W images, whereas amino acid PET uptake reflects tumour metabolism related to over-expression of L-type amino acid transporters in the cell membrane.

Our results are similar to those reported by other groups. Ledezma et al. [18] demonstrated that fusion technology on separate machines helps the precise localisation of ^{18}F -DOPA activity in primary and recurrent tumours: ^{18}F -DOPA PET appeared to be highly sensitive for gliomas, irrespective of tumour grade, labelling both enhancing and non-enhancing tumour equally well. Similarly, Karunanithi et al. evaluated the diagnostic accuracy of contrast-

enhanced (Ce) MRI and ^{18}F -DOPA PET-CT for detection of recurrent glioma and found ^{18}F -DOPA to be more specific than Ce-MRI for both high-grade and low-grade tumours [19].

Two other studies [13, 20] have compared the feasibility of dynamic studies with amino acid tracers and multiparametric MRI on a single PET/MRI machine but to our knowledge no studies have as yet investigated the added value of ^{18}F -DOPA PET/MRI in assessing treatment response. In our study, we found an increase in the AUC using the PET/MRI multiparametric approach compared with MRI alone.

One of the questions we sought to answer was the extent of the correlation between ^{18}F -DOPA PET and MRI volumes and areas of overlap. To our knowledge this is the first study to examine these features on a hybrid scanner.

Our results showed that the volume of residual disease at ^{18}F -DOPA PET was larger for HGGs than for LGGs compared with MR volumes. Moreover, the percentage of overlap was significantly higher for LGGs than for HGGs. While it is not possible to confirm the accuracy of our results, i.e. our results were not confirmed with targeted biopsies at the level of areas of uptake and signal change on tumours, this finding could be clinically relevant if confirmed by larger cohort studies as it would allow better target identification for radiotherapy planning [more accurate definition of clinical target volume (CTV extension)]. This would be particularly true in the case of HGGs, where the concordance with MRI volumes was lower.

The second aim of our study was to investigate the possible role of ^{18}F -DOPA in the evaluation of residual disease, compared with MRI. It is known that MRI is of limited value in assessing the presence of residual active disease in non-enhancing tumours after treatment. In our cohort, when the values of SUV_{max} in different tumour components were plotted against the CBV values derived from the DSC-PWI, PET was better able to differentiate components within the lesion as they exhibited different metabolic activity. By contrast, CBV_{mean} values (Figure 3) usually overlapped; indeed, PET allowed the demonstration of foci of active disease (uptake) even in non-enhancing regions. It is important to note that the combination of PET with MRI on a single hybrid platform, with simultaneous acquisition of imaging, allows better image registration and more reliable results than does separate imaging acquisition.

The qualitative assessment in our study showed agreement between the modalities in most patients; out of three discordant cases, two were positive on MRI but negative on PET while

one was positive on PET but negative on MRI. Biopsy of these cases demonstrated presence of tumour in all cases. It is hard to identify the reasons for these discordances. In the negative PET cases, the lesions on MRI were non-enhancing, with limited alteration of perfusion values (Figure 4). The negative MRI case was, by contrast, a complex case where the radiologists considered a focal area of enhancement (with low-grade perfusion) to represent radionecrosis (considered negative on the database). This lesion was focally positive on PET (Figure 5) and was interpreted as an active tumour at follow-up since it increased progressively in size, even beyond 12 months after radiotherapy, with worsening of the patient's clinical condition.

Assessment of the accuracy of PET, MRI and multiparametric PET/MRI through ROC analysis confirmed an improved AUC for the diagnosis of active disease using the hybrid technique, similar to the observations of Pika et al. [20]. However, it could be argued that assessing the accuracy may be a challenging task since it can be influenced by the multiparametric PET/MRI protocol (with many clinical and technical factors potentially affecting the results), the chosen cohort and the way in which the data are analysed. In this study, we performed a simple evaluation of the multiparametric data by analysing a linear combination of the parameters correlated to the final diagnosis of presence of active tissue. We acknowledge that our approach did not take into account either important clinical variables (e.g. the presence of pseudo-progression or radionecrosis) or more advanced MRI sequences (e.g. spectroscopy, ASL or modelled DWI), which certainly can influence the value of a multimodality approach. Nevertheless, one of the peculiarities/clinical advantages of ^{18}F -DOPA is the rapid uptake during the first minutes after injection: tumour tracer uptake is highest at between 10 and 30 min after injection, after which it declines. Accordingly, the scan time is relatively short and the MRI sequences are rapid. While other PET tracers, e.g. ^{18}F -FET, have a longer uptake time that allows for longer MRI sequences and therefore acquisition of a more comprehensive MR exam, this may prove counterproductive in non-cooperative patients or those with a suboptimal performance status.

We recognise that our study has some limitations. First, we did not evaluate ^{18}F -DOPA PET with respect to other extra MRI sequences that may provide additional information (e.g. ADC for degree of tumour cellularity, oxygen-enhanced MRI for hypoxia or spectroscopy for metabolite concentrations) and we did not have confirmation of residual disease with targeted biopsies at the level of areas of uptake and signal change. However, larger tumour volumes on ^{18}F -DOPA PET than on MRI, both in enhancing and non-enhancing regions, have already

been reported, suggesting that PET volumes correlate better with the real tumour extension [21, 24]; additionally, it is worth to say that combined modalities (fused PET/CT and MRI or PET/MRI) have already been proven to offer advantages over separate PET/CT and MRI, for instance in the evaluation of the striatal involvement in glioma in children [25, 26].

Secondly, we acknowledge that the ROC curves may have been inflated by the use of a simple dichotomous evaluation of presence or absence of active disease, without taking into consideration other important relevant information. This approach was chosen because the primary aim of our study was to identify volumetric differences in tumours with the clinical intent of providing guidance for radiotherapy planning. Recently, Pika et al. [20] focussed their study on this specific point, undertaking a more thorough analysis. These authors demonstrated that hybrid dynamic ^{18}F -FET PET/MRI adds value in distinguishing between recurrence and treatment-related changes, with a trend similar to that observed in this paper.

Lastly, we recognise that patients received different treatments (radiotherapy, chemotherapy, surgery), but this reflects what usually happens in routine clinical practice. Prospective studies with more homogeneous cohorts are envisaged to evaluate the efficacy of the hybrid technique with regard to specific treatments.

Conclusion

We found that the complementary use of PET/MRI may help in assessing response to treatment in non-enhancing tumours, compared to cross-sectional MRI alone. Additional information provided by ^{18}F -DOPA PET/MRI for evaluation of different features of the tumour and assessment of the glioma burden may help to improve care, optimise neuro-oncology outcomes and allow more focussed therapies, especially in fragile patients (e.g. paediatric patients).

References

1. Wen PY, Macdonald DR, Reardon DA et-al. Updated response assessment criteria for high-grade gliomas: response assessment in neuro-oncology working group. *J. Clin. Oncol.* 2010;28 (11): 1963-72. doi:10.1200/JCO.2009.26.3541.
2. Lin NU, Lee EQ, Aoyama H, Barani IJ, Baumert BG, et al.; Response Assessment in Neuro-Oncology (RANO) group. Challenges relating to solid tumour brain metastases in clinical trials, part 1: patient population, response, and progression. A report from the RANO group. *Lancet Oncol.* 2013 Sep;14(10):e396-406. doi:10.1016/S1470-2045(13)70311-5. Review. PubMed PMID: 23993384.
3. Quant EC, Wen PY. Response assessment in neuro-oncology. *Curr Oncol Rep.* 2011 Feb;13(1):50-6. doi: 10.1007/s11912-010-0143-y. Review. PubMed PMID: 21086192.
4. Ellingson B. M., Kim H. J., Woodworth D. C., Pope W. B., Cloughesy J. N., Harris R. J. et al. Recurrent Glioblastoma Treated with Bevacizumab: Contrast-enhanced T1-weighted Subtraction Maps Improve Tumor Delineation and Aid Prediction of Survival in a Multicenter Clinical Trial.: *Radiology*, 2014, Vol. 271.
5. Benjamin M. Ellingson, Patrick Y. Wen and Timothy F. Cloughesy. Modified Criteria for Radiographic Response Assessment in Glioblastoma Clinical Trials. *Neurotherapeutics*, 2017, Vol. 14.
6. Nathalie L. Albert, Michael Weller, Bogdana Suchorska, Norbert Galldiks, Riccardo Soffietti, Michelle M. Kim, Christian la Fougère, Whitney Pope, Ian Law, Javier

Arbizu Marc C., Chamberlain Michael, Vogelbaum, Ben M. Ellingson, Joerg C. Tonn. Response Assessment in Neuro-Oncology working group and European Association for Neuro-Oncology recommendations for the clinical use of PET imaging in gliomas. 9, s.l. : Neuro-Oncology, 2016, Vol. 18.

7. Morana G, Piccardo A, Puntoni M, et al. Diagnostic and prognostic value of 18F-DOPA PET and 1H-MR spectroscopy in pediatric supratentorial infiltrative gliomas: a comparative study. *Neuro Oncol.* 2015 Dec;17(12):1637-47. doi:10.1093/neuonc/nov099.
8. Zaccagna F, Riemer F, Priest AN, McLean MA, et al. Non-invasive assessment of glioma microstructure using VERDICT MRI: correlation with histology. *Eur Radiol.* 2019 Mar 19. doi: 10.1007/s00330-019-6011-8.
9. Morana G, Piccardo A, Tortora D, et al. Grading and outcome prediction of pediatric diffuse astrocytic tumors with diffusion and arterial spin labeling perfusion MRI in comparison with 18F-DOPA PET. *Eur J Nucl Med Mol Imaging.* 2017 Nov;44(12):2084-2093. doi: 10.1007/s00259-017-3777-2.
10. Almansory KO, Fraioli F. Combined PET/MRI in brain glioma imaging. *Br J Hosp Med (Lond).* 2019 Jul 2;80(7):380-386. doi: 10.12968/hmed.2019.80.7.380.
11. Mansoor NM, Thust S, Militano V, Fraioli F. PET imaging in glioma: techniques and current evidence. *Nucl Med Commun.* 2018 Dec;39(12):1064-1080. doi: 10.1097/MNM.0000000000000914.
12. Boscolo Galazzo I, Mattoli MV, Pizzini FB, De Vita E, Barnes A, Duncan JS, Jäger HR, Golay X, Bomanji JB, Koepp M, Groves AM, Fraioli F. Cerebral metabolism and perfusion in MR-negative individuals with refractory focal epilepsy assessed by

simultaneous acquisition of (18)F-FDG PET and arterial spin labeling. *Neuroimage Clin.* 2016 Apr 12;11:648-657. doi: 10.1016/j.nicl.2016.04.005.

13. Pafundi DH, Laack NN, Youland RS, et al. Biopsy validation of 18F-DOPA PET and biodistribution in gliomas for neurosurgical planning and radiotherapy target delineation: results of a prospective pilot study. *Neuro Oncol.* 2013 Aug;15(8):1058-67. doi: 10.1093/neuonc/not002.
14. Kosztyla R, Chan EK, Hsu F, Wilson D, et al. High-grade glioma radiation therapy target volumes and patterns of failure obtained from magnetic resonance imaging and 18F-FDOPA positron emission tomography delineations from multiple observers. *Int J Radiat Oncol Biol Phys.* 2013 Dec 1;87(5):1100-6. Doi 10.1016/j.ijrobp.2013.09.008.
15. Patel CB, Fazzari E, Chakhoyan A, Yao J, Raymond C, Nguyen H, et al. (18)F-FDOPA PET and MRI characteristics correlate with degree of malignancy and predict survival in treatment-naïve gliomas: a cross-sectional study. *J Neurooncol.* 2018 Sep;139(2):399-409. doi: 10.1007/s11060-018-2877-6.
16. Karunanithi S, Sharma P, Kumar A, Khangembam BC, Bandopadhyaya GP, et al. Comparative diagnostic accuracy of contrast-enhanced MRI and (18)F-FDOPA PET-CT in recurrent glioma. *Eur Radiol.* 2013 Sep;23(9):2628-35. doi: 10.1007/s00330-013-2838-6.
17. Weber MA, Henze M, Tüttenberg J, Stieltjes B, Meissner M, et al. Biopsy targeting gliomas: do functional imaging techniques identify similar target areas? *Invest Radiol.* 2010 Dec;45(12):755-68. doi:10.1097/RLI.0b013e3181ec9db0.

18. Verger A, Filss CP, Lohmann P, Stoffels G, Sabel M, Wittsack HJ, et al. Comparison of O-(2-(18)F-Fluoroethyl)-L-Tyrosine Positron Emission Tomography and Perfusion-Weighted Magnetic Resonance Imaging in the Diagnosis of Patients with Progressive and Recurrent Glioma: A Hybrid Positron Emission Tomography/Magnetic Resonance Study. *World Neurosurg.* 2018 May;113:e727-e737. doi: 10.1016/j.wneu.2018.02.139.
19. Jena A, Taneja S, Gambhir A, Mishra AK, D'souza MM, et al. Glioma Recurrence Versus Radiation Necrosis: Single-Session Multiparametric Approach Using Simultaneous O-(2-18F-Fluoroethyl)-L-Tyrosine PET/MRI. *Clin Nucl Med.* 2016 May;41(5):e228-36. doi: 10.1097/RLU.0000000000001152.
20. Jena A, Taneja S, Jha A, Damesha NK, Negi P, Jadhav GK, Verma SM, Sogani SK. Multiparametric Evaluation in Differentiating Glioma Recurrence from Treatment-Induced Necrosis Using Simultaneous (18)F-FDG-PET/MRI: A Single-Institution Retrospective Study. *AJNR Am J Neuroradiol.* 2017May;38(5):899-907. doi: 10.3174/ajnr.A5124.
21. David N. Louis, Arie Perry, Guido Reifenberger, Andreas von Deimling, Dominique Figarella-Branger, Webster K. Cavenee, Hiroko Ohgaki, Otmar D. Wiestler, Paul Kleihues, David W. Ellison. The 2016 World Health Organization Classification of Tumors of the Central Nervous System: a summary. *Acta Neuropathologica*, 2016, Vol. 131
22. Vander Borgh T., Asenbaum S., Bartenstein K., Halldin C., Kapucu Ö., Van Laere K, Varrone A., Tatsch K. *EANM Procedure Guidelines for Brain Tumour Imaging using labelled Amino Acid Analogues.* *Eur J Nucl Med Mol Imaging.*, 2006, Vol. 33.

23. VASARI Project. *wiki.cancerimagingarchive.net*. [Online] 2016.
<http://wiki.cancerimagingarchive.net>.
24. Ledezma CJ, Chen W, Sai V, Freitas B, Cloughesy T, Czernin J, Pope W. 18F-FDOPA PET/MRI fusion in patients with primary/recurrent gliomas: initial experience. *Eur J Radiol*. 2009 Aug;71(2):242-8. doi: 10.1016/j.ejrad.2008.04.018.
25. Karunanithi S, Sharma P, Kumar A, Khangembam BC, Bandopadhyaya GP, Kumar R, Goenka A, Gupta DK, Malhotra A, Bal C. Comparative diagnostic accuracy of contrast-enhanced MRI and (18)F-FDOPA PET-CT in recurrent glioma. *Eur Radiol*. 2013 Sep;23(9):2628-35. doi: 10.1007/s00330-013-2838-6.
26. Pyka T, Hiob D, Preibisch C, Gempt J, Wiestler B, Schlegel J, Straube C, Zimmer C. Diagnosis of glioma recurrence using multiparametric dynamic 18F-fluoroethyl-tyrosine PET-MRI. *Eur J Radiol*. 2018 Jun;103:32-37. doi: 10.1016/j.ejrad.2018.04.003.
27. Verger A, Filss CP, Lohmann P, Stoffels G, Sabel M, Wittsack HJ, et al. Comparison of (18)F-FET PET and perfusion-weighted MRI for glioma grading: a hybrid PET/MR study. *Eur J Nucl Med Mol Imaging*. 2017 Dec;44(13):2257-2265. doi: 10.1007/s00259-017-3812-3.
28. Deanna H. Pafundi, Nadia N. Laack, Ryan S. Youland, Ian F. Parney, Val J. Lowe, et al. Biopsy validation of 18F-DOPA PET and biodistribution in gliomas for neurosurgical planning and radiotherapy target delineation: results of a prospective pilot study. 8, s.l. : Neuro Oncology, 2013, Vol. 15.

Morana G, Puntoni M, Garrè ML, Massollo M, et al. Ability of (18)F-DOPA PET/CT and fused (18)F-DOPA PET/MRI to assess striatal involvement in paediatric glioma. Eur J Nucl Med Mol Imaging. 2016 Aug;43(9):1664-72. doi:10.1007/s00259-016-3333-5. Epub 2016 Feb 25.

Tables

Table 1: Characteristics of the enrolled patients (n=40)

Table 2: MRI and PET features. Figures are expressed as median (interquartile range 1–3). Enhancement was scored from 0 to 5 using the VASARI scoring system. Volume is expressed in mm³

Table 3: PET features according to presence of MRI enhancement. Figures are expressed as median (interquartile range 1–3)

Figure Captions

Figure 1. Sample slices for one WHO grade 4 patient to evaluate the overlap of the tumour volumes drawn manually on both modalities

Figure 2. Correlation matrix for: size of tumour (longest and perpendicular), SUV_{max} , T/N, T/S, degree of enhancement, CBV_{mean} , CBV_{max} , CBF_{mean} and CBF_{max} . Correlations were explored using the Spearman's correlation coefficient; to account for multiple comparison the Bonferroni correction was applied. A value of 1 expresses a complete positive correlation; a value of -1 expresses a complete negative correlation. Highlighted cells indicate statistical significance

Figure 3. Distribution of uptake (SUV_{max}) over CBV_{mean} among different ROIs in the enhancing (red), non-enhancing (green), necrotic (blue) and normal white matter (purple). The ovals of the same colours with the parameters show a multivariate t -distribution

Figure 4. Multimodal imaging of residual tumour: 35-year old patient with anaplastic astrocytoma (WHO III) 12 months after resection and radiation therapy. Structural MRI (A, B) show a solid lesion in the resection cavity, without contrast enhancement (C). Perfusion MRI (D, red circle) shows mild increased perfusion in this area, suggesting vital tumour tissue. ^{18}F -DOPA PET shows no increased uptake in this area. In this case the gold standard was surgical biopsy.

Figure 5. DSC-PWI (right) and ^{18}F -DOPA PET fused with T1 contrast-enhanced MRI. DSC-PWI shows limited perfusion (red circle) despite intense ^{18}F -DOPA uptake at the corresponding level. The gold standard in this case, surgical biopsy, demonstrated active recurrent disease.

Funding:

This work was taken at UCLH/UCL which received a proportion of funding from the UK's Department of Health's NIHR Biomedical Centres (BRC UCLH 2012) funding scheme.

Dr. Fuad Novruzov is supported by funding from the Science Development Foundation under the President of the Republic of Azerbaijan [Grant № EIF/GAM-4-BGM-GIN-2017-3(29)-19/13/3].

Compliance with ethical standards

There is no Disclosure with this paper. The sponsors had no role in the design of the study, the collection and analysis of the data, or in the preparation of the manuscript.

Ethical approval

All procedures performed in studies involving human participants were in accordance with the ethical standards of the institutional and/or national research committee and with the 1964 Helsinki Declaration and its later amendments or comparable ethical standards.

Informed consent: *Informed consent was obtained from all individual participants included in the study.*

Acknowledgements:

The authors want to acknowledge the help of Anna Barnes PhD and Marilena Rega for their contribution to the image reconstruction at the Institute of Nuclear Medicine, London, UK.

We would also like to acknowledge Dr. Stefan Voo, Dr. Zhangjie Su and Dr Nigar Aliyeva, for helping with the Database and clinical information of patients.

In addition, we would like to thank Prof. Jamil A. Aliyev for the successful conduct of the study and with the supporting and granting the visiting fellowship of Dr. Fuad Novruzov at the University College London Hospitals.

Table 1: Patients' characteristics

		Frequency		Percentage (%)
Parameters	Group	(number)		
Sex	M	23		60
	F	17		40
Age	5-65 yo			
	34 (median)			
WHO Grade	I	3		7.5
	II	12		30.0
	III	14		35.0
	IV	11		27.5
Type of Glioma	Glioblastoma multiforme (GBM)			
		11		27
	Astrocytoma			
		23		57
Treatment	Oligodendroglioma			
		6		15
	chemo-radiation			
		26		65.0
	radiotherapy			
		8		20.0
	surgery			
		1		2.5
	chemotherapy			
		5		12.5

Table 2: MRI and PET

Features	Low Grade		High Grade
Parameters			
Size (mm)	32.9		
	(24.75-	31.0	(22.0-
	48.60)		41.2)
Median and IQR			
Enhancement	0	6	5
	1	1	2
	2	1	5
	3	3	6
	4	1	5
	5	3	2
Necrosis		6	13
SUVmax	3.40		3.3
	(2.2-4.0)		(2.7-4.8)
T/S	1.35		1.80
	(1.3-1.625)		(1.375-2.0)
T/N	1.80		2.55
	(1.6-3.1)		(2.075-2.8)
Vol MRI	5931.55		6316.57
	(4161.13-		(4210.24-
	8929.32)		13986.00)
Vol Fdopa	6284.94		8216.88
	(4610.00-		(5973.00-
	8960.99)		19300.00)
Perfusion rCBV	1.28		1.70

(0.787-	(1.573-
1.517)	2.12975)

Table 3: PET Features	Non-enhancing lesions	Enhancing lesions
Parameters		
SUVmax	2.50	3.95
Median and IQR	(2.225-3.375)	(3.05-5.025)
T/S	1.30	1.80
Median and IQR	(1.30-1.40)	(1.40-2.00)
T/N	1.85	2.60
Median and IQR	(1.70-2.50)	(2.10-3.00)

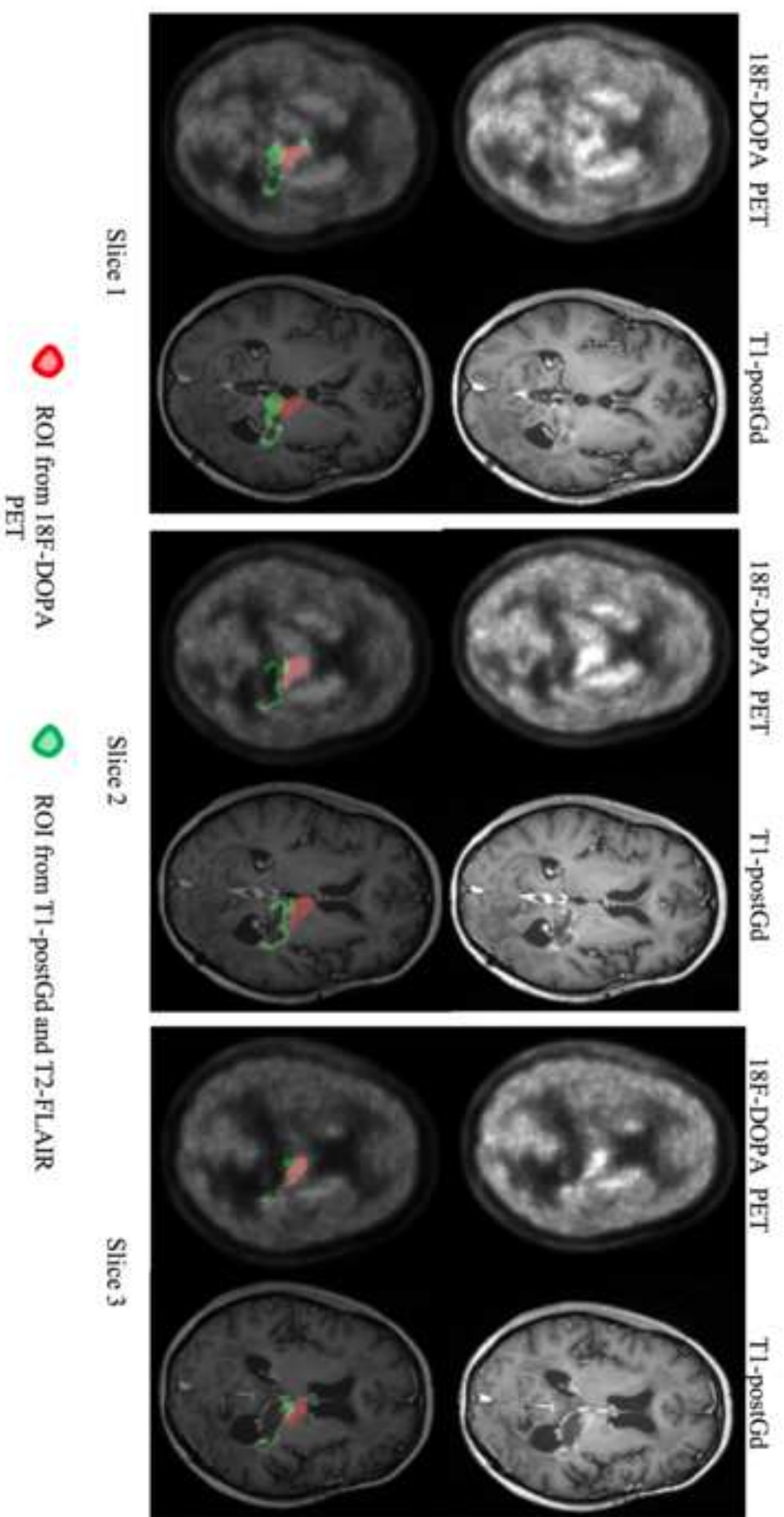


figure 2

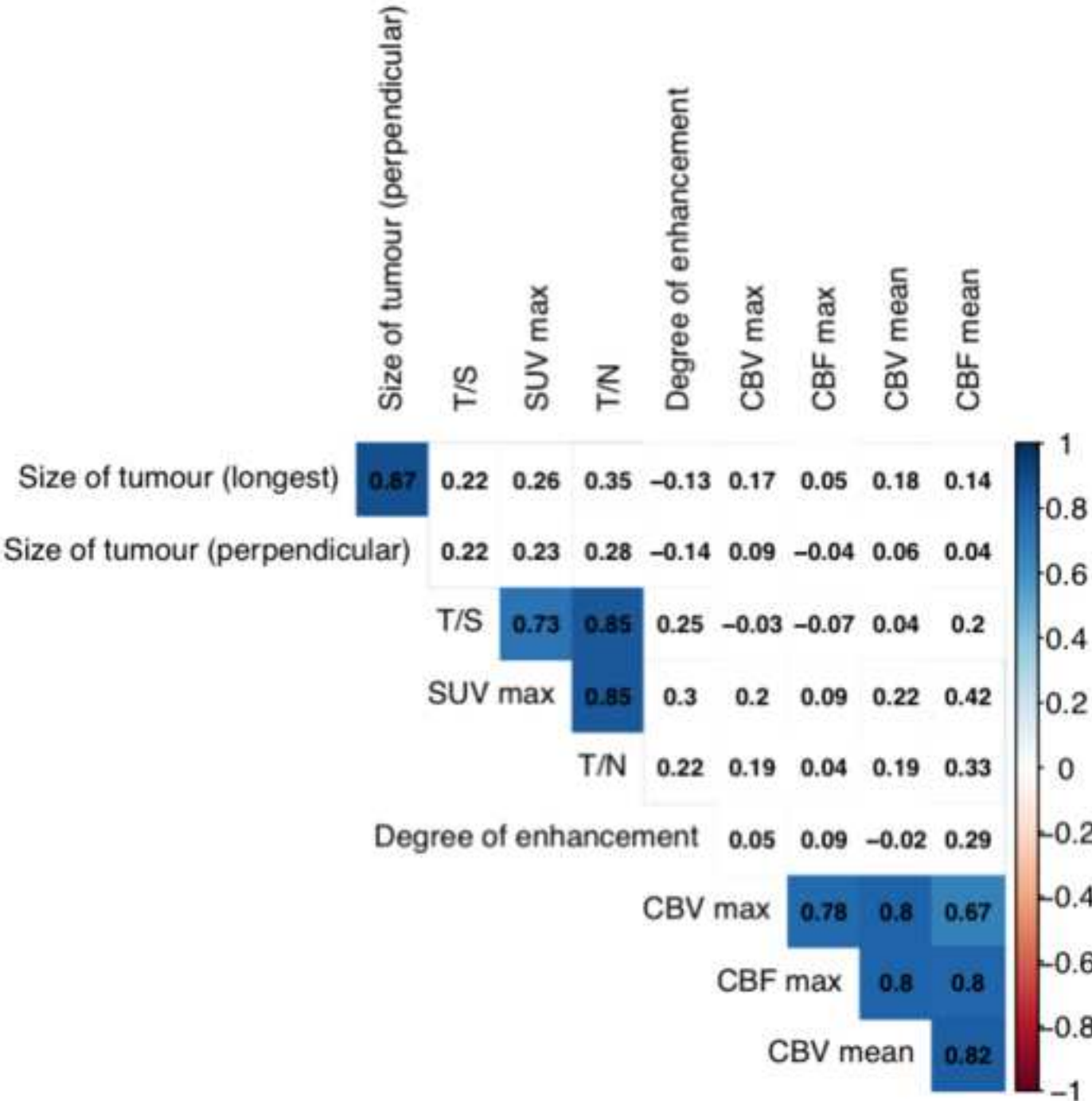


figure 3

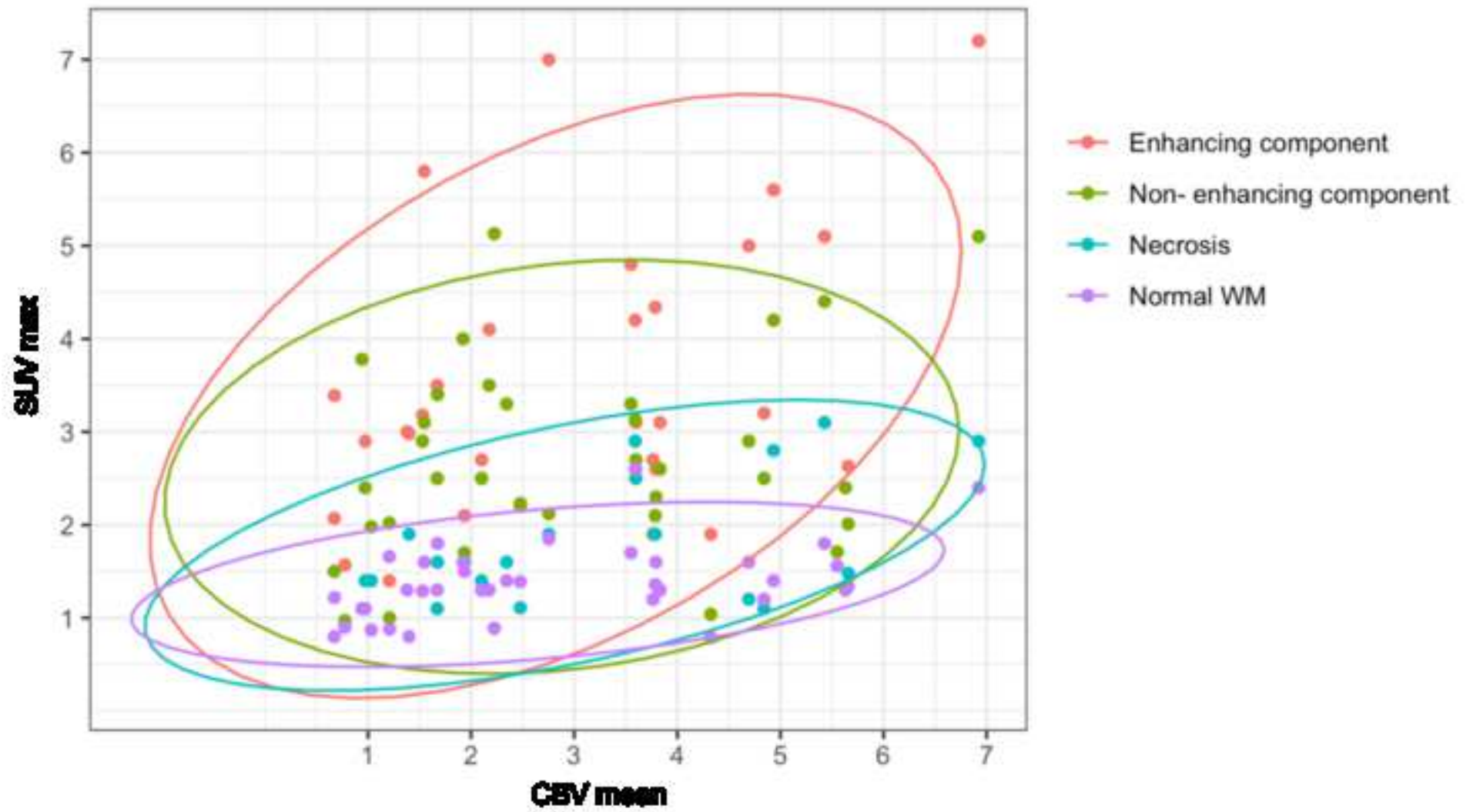


figure 4

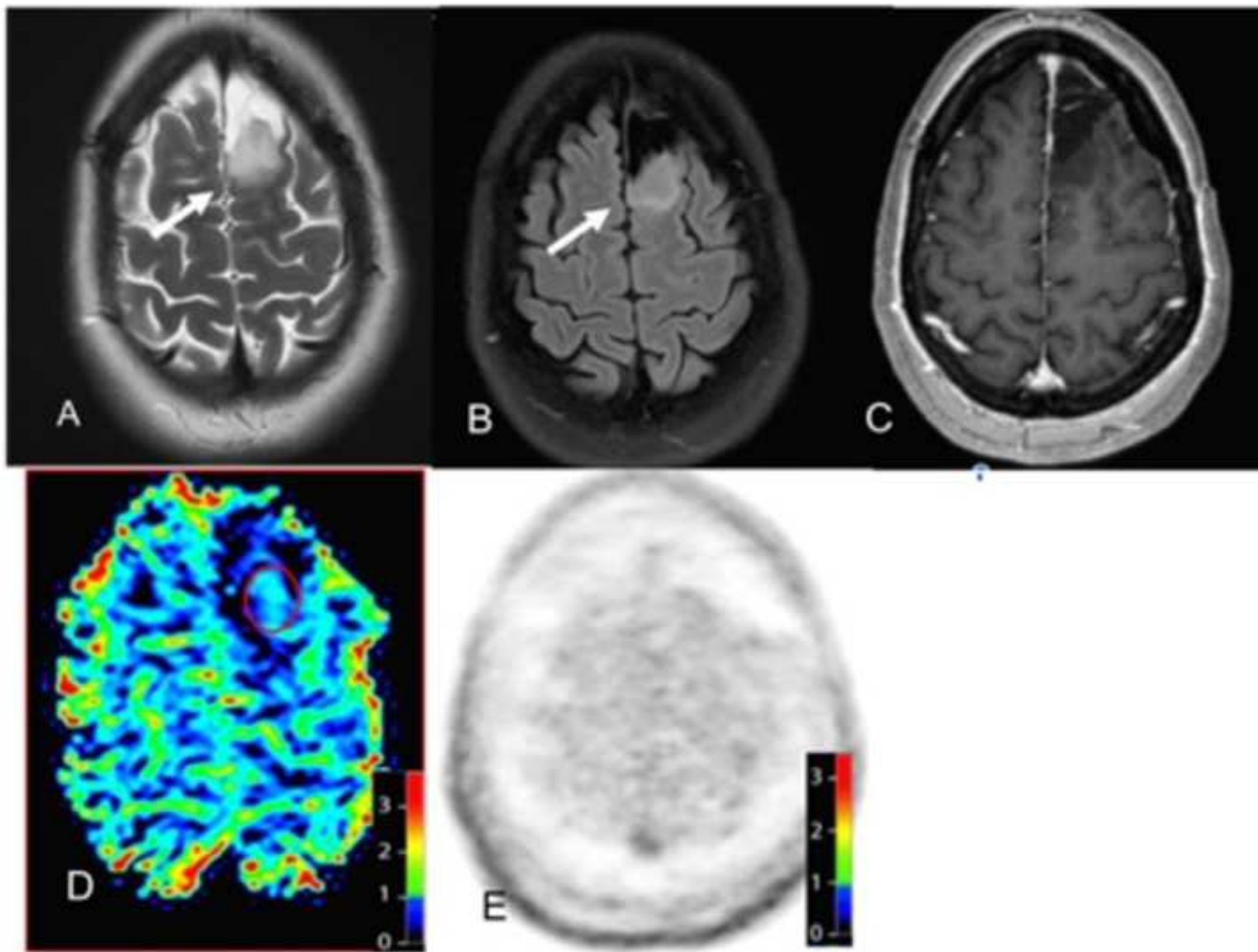


figure 5

